

Ambiguity function and accuracy of the hyperbolic chirp: comparison with the linear chirp

Alessio Balleri[#] and Alfonso Farina^{*}

Abstract

In this paper, we derive the Ambiguity Function (AF) of a narrowband and a wideband hyperbolic chirp. We calculate the second derivatives of the squared amplitude of the narrowband Complex Ambiguity Function (CAF) and use them to calculate the Fisher Information Matrix (FIM) of the estimators of the target range and velocity. The FIM is then used to calculate the Cramér-Rao Lower Bounds (CRLB) of the variance of the estimators and to carry out an analysis of estimation performance and a comparison with the case of a linear chirp with a rectangular and a Gaussian amplitude modulation. The analysis and the calculations of the CRLB are also extended to a train of hyperbolic chirps. Results corroborate that at narrowband the hyperbolic chirp is less Doppler tolerant than the linear chirp and show that the hyperbolic chirp provides a comparable measurement accuracy to the linear chirp. Results at wideband corroborate the superior Doppler tolerance of the hyperbolic chirp with respect to that of the linear chirp.

Index Terms

Hyperbolic Chirp, Bat Echolocation Waveform, Radar Waveform, Ambiguity Function, Fisher Information Matrix, CRLB, narrowband, wideband.

I. INTRODUCTION

The ability to jointly and accurately estimate the distance and the velocity of a target using one or multiple consecutive echoes has attracted considerable interest in the radar and sonar community. The first studies on this topic were carried out for narrowband signals in white noise, e.g. in [1] and [2], and these were then extended to the Maximum Likelihood estimates of the target parameters for an antenna array in [3]. The more general expressions for the CRLB of the Direction of Arrival (DoA), target range and target Doppler for an antenna array at narrowband and in non-white noise were derived and presented in [4]. In this same paper, the authors extended their results to the case of a train of linear chirps with large time-bandwidth products.

Hyperbolic chirps have attracted considerable research interest in the past because of their Doppler tolerance properties. They were initially proposed to increase the receiver Doppler tolerance in sonar as well as radar detecting

[#]A. Balleri, Centre for Electronic Warfare, Cranfield University, Defence Academy of the UK, Shrivenham, SN6 8LA, UK, e-mail: a.balleri@cranfield.ac.uk.

^{*}A. Farina, Consultant, Selex ES (Retired), Rome, Italy, e-mail: alfonso.farina@outlook.it

high-velocity targets with large time-bandwidth products [5]. A second order Taylor series expansion was used in [6] to study the properties of the main lobe of the AF of the hyperbolic chirp and the same paper presents an analysis of the Doppler tolerance for a train of hyperbolic chirps. In [7], it was shown that the hyperbolic frequency modulation is the optimal modulation, in terms of Doppler tolerance, for applications that require a large time-bandwidth product (e.g. for space applications of radar, targets can reach velocities of over 9,000 m/s and time-bandwidth products greater than about 16,000 are to be considered large). The same paper contains the derivation of the Fourier transform of the hyperbolic chirp and a study of the shape and properties of its cross-correlation function. A nice technical report that summarises the properties of the hyperbolic chirp can be found in [8].

The existing literature has also focused on techniques to estimate the parameters of signals with a hyperbolic frequency modulation. The estimators of the parameters of a class of discrete signals with an hybrid FM-polynomial phase modulation and their relative CRLBs were developed in [9], [10] and [11]. In these papers, the authors studied the hyperbolic chirp as a special case of an hybrid FM-polynomial signal and found that the ambiguity function of the hyperbolic chirp tends to a Dirac Delta function when the number of elements of the signal grows without limit.

Some species of bats have developed an excellent ability to echolocate to search, detect and localise their prey. They do this by transmitting sophisticated ultrasound waveforms and by using target echoes to gather an acoustic picture of the surrounding environment. Previous research and experiments have shown that bat echolocation calls often present a hyperbolic-like frequency modulation, in particular when the bat forages on flying insects in a highly cluttered environment [12]. The knowledge of the estimation performance of the target range and velocity as a function of the design of the hyperbolic chirp can potentially help underpin the relationships between the insect flight trajectory, the waveforms used by the bat and how these are diversified during a mission [13] [14] [15].

This paper is organised as follows; in Section II we calculate the AF of a narrowband hyperbolic chirp, in Section III we derive the FIM of the target range and velocity estimators and derive the CRLB of their variance as a function of the Signal to Noise Ratio (SNR), in section IV we compare the performance of the hyperbolic chirp with respect to a Linearly Frequency Modulated chirp (LFM) with a rectangular and a Gaussian amplitude modulation, in section V we extend the calculation of the CRLBs to a train of pulses and carry out a comparison with a train of LFM chirps, in section VI the AFs of the waveforms are compared to facilitate the interpretation of the results, and finally in section VII we derive the AF of the wideband hyperbolic chirp before drawing the conclusions in section VIII. All the calculations are given in detail in the Appendices A, B, C and D.

II. NARROWBAND AMBIGUITY FUNCTION OF THE HYPERBOLIC CHIRP

Consider the analytical signal $\hat{s}(t)$ of a narrowband hyperbolic chirp of unit energy and duration T

$$\hat{s}(t) = s(t)e^{j2\pi f_0 t} = \frac{1}{\sqrt{(T)}} e^{j2\pi a \ln(1+kt)} \text{Rect}\left\{\frac{t}{T}\right\} e^{j2\pi f_0 t} \quad (1)$$

with the function $\text{Rect}\left\{\frac{t}{T}\right\}$ being a rectangular function of the time variable t such that

$$\text{Rect}\left\{\frac{t}{T}\right\} = \begin{cases} 1 & 0 < t < T \\ 0 & \text{elsewhere} \end{cases}$$

The instantaneous frequency of the chirp

$$f(t) = \frac{1}{2\pi} \frac{d(2\pi a \ln(1 + kt))}{dt} + f_0 = \frac{ak}{1 + kt} + f_0 \quad (2)$$

is a function of the parameters a and k which define the design of the baseband hyperbolic chirp, and that depend on the start and end frequencies, $f_1 = f(0) - f_0$ and $f_2 = f(T) - f_0$, of the complex envelope $s(t)$. These can be calculated according to the relation

$$\begin{cases} f_1 = ak \\ k = \frac{f_1 - f_2}{T f_2} \end{cases}$$

The Complex Ambiguity Function (CAF) is defined as [16]

$$\chi(\tau, \nu) = \int_{-\infty}^{\infty} s(t) s^*(t + \tau) e^{j2\pi\nu t} dt \quad (3)$$

and for the hyperbolic chirp and $0 < \tau < T$ can be written in the form ¹

$$\chi(\tau, \nu) = \frac{1}{T} \int_0^{T-\tau} e^{j2\pi a \ln(1+kt)} e^{-j2\pi a \ln(1+k(t+\tau))} e^{j2\pi\nu t} dt \quad (4)$$

Using the equality $e^{j \ln x} = x^j$ we rewrite the integral as

$$\chi(\tau, \nu) = \frac{1}{T} \int_0^{T-\tau} (1 + kt)^{j2\pi a} (1 + k(t + \tau))^{-j2\pi a} e^{j2\pi\nu t} dt \quad (5)$$

which after the change of variable $t_1 = kt$ becomes

$$\chi(\tau, \nu) = \frac{1}{kT} \int_0^{k(T-\tau)} (1 + t_1)^{j2\pi a} (t_1 + (1 + k\tau))^{-j2\pi a} e^{j\frac{2\pi\nu}{k} t_1} dt_1 \quad (6)$$

We then apply a further change of variable $t_1 = k(T - \tau)w$ that leads to

$$\chi(\tau, \nu) = \frac{(T - \tau)}{T(1 + k\tau)^{j2\pi a}} \int_0^1 (1 - k(\tau - T)w)^{j2\pi a} \left(1 - \frac{k(\tau - T)}{(1 + k\tau)} w\right)^{-j2\pi a} e^{j2\pi\nu(T-\tau)w} dw \quad (7)$$

and define the parameters

$$\begin{cases} \gamma = j2\pi a \\ u = k(\tau - T) \\ q = \frac{k(\tau - T)}{(1 + k\tau)} \\ \beta = j2\pi\nu(T - \tau) \end{cases}$$

to obtain a simplified form of the integral

$$\chi(\tau, \nu) = \frac{(T - \tau)}{T(1 + k\tau)^{j2\pi a}} \int_0^1 (1 - uw)^\gamma (1 - qw)^{-\gamma} e^{\beta w} dw \quad (8)$$

For $\nu = 0$, $\beta = 0$ and the integral becomes

$$\chi(\tau, 0) = \frac{(T - \tau)}{T(1 + k\tau)^{j2\pi a}} \int_0^1 (1 - uw)^\gamma (1 - qw)^{-\gamma} dw \quad (9)$$

¹The integral is solved for $\tau > 0$ without loss of generality.

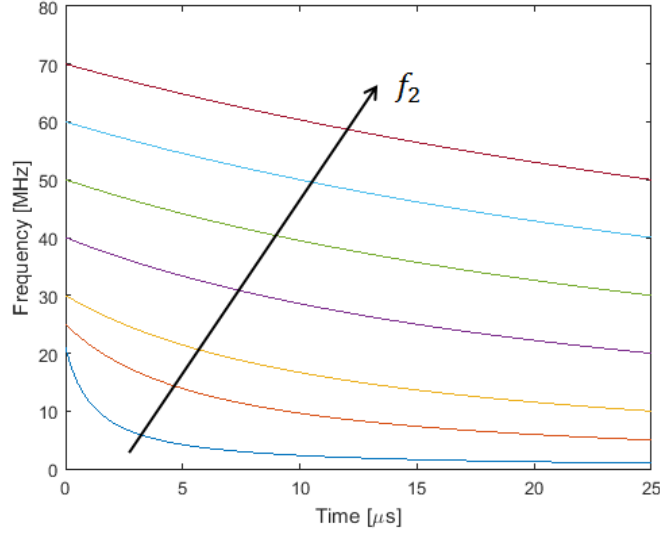


Fig. 1. Change in curvature as a function of the parameter f_2 for a hyperbolic chirp of bandwidth $B = 20$ MHz and duration $25 \mu s$.

which represents the autocorrelation of the hyperbolic chirp. The integral in Eq. 9 is of a known form and can be solved as

$$\chi(\tau, 0) = \frac{(T - \tau)}{T(1 + k\tau)^{j2\pi a}} B(1, 1) F_1(1, -\gamma, \gamma, 2; u, q) \quad (10)$$

by recalling the equality given in Appendix A [17], which converges² for $|u| < 1$ and $|q| < 1$. It is simple to show that these conditions are verified when the lower frequency of the hyperbolic chirp is greater than the chirp bandwidth, i.e. when $f_2 > B$. In the equation, the function $B(x, y)$ is a Beta function and the function $F_1(a, b_1, b_2, c; x, y)$ is an hypergeometric function of two variables, also known as the Appell series [18]. Fig. 1 shows the impact that the conditions on $|u|$ and $|q|$ have on the curvature of the hyperbolic chirps of a given bandwidth and duration. The plot shows how the curvature of the chirp changes when f_2 increases and shows that with the increase in f_2 the hyperbolic transition becomes more and more linear.

To the best of our knowledge the integral in Eq. 8 is unknown but it can be approximated by replacing the term $e^{\beta w}$ with a Taylor series expansion as

$$\chi(\tau, \nu) = \frac{(T - \tau)}{T(1 + k\tau)^{j2\pi a}} \sum_{n=0}^{\infty} \frac{\beta^n}{n!} \int_0^1 w^n (1 - uw)^\gamma (1 - qw)^{-\gamma} dw \quad (11)$$

By using the same equality given in Appendix A, the terms of the series can be written as a function of the same hypergeometric function of two variables as

$$\chi(\tau, \nu) = \frac{(T - \tau)}{T(1 + k\tau)^{j2\pi a}} \sum_{n=0}^{\infty} \frac{\beta^n}{n!} B(n + 1, 1) F_1(n + 1, -\gamma, \gamma, n + 2; u, q) \quad (12)$$

²The table of integrals in [17] indicates that the integral converges for $|u| < 1$ and $|q| < 1$. It is simple to show that these conditions are verified when the lower frequency of the hyperbolic chirp is greater than the chirp bandwidth ($f_2 > B$). However, it is a property of the Ambiguity Function that $|\chi(\tau, \nu)| \leq |\chi(0, 0)| = 1$ and this implies the condition on the tables is only sufficient but not necessary.

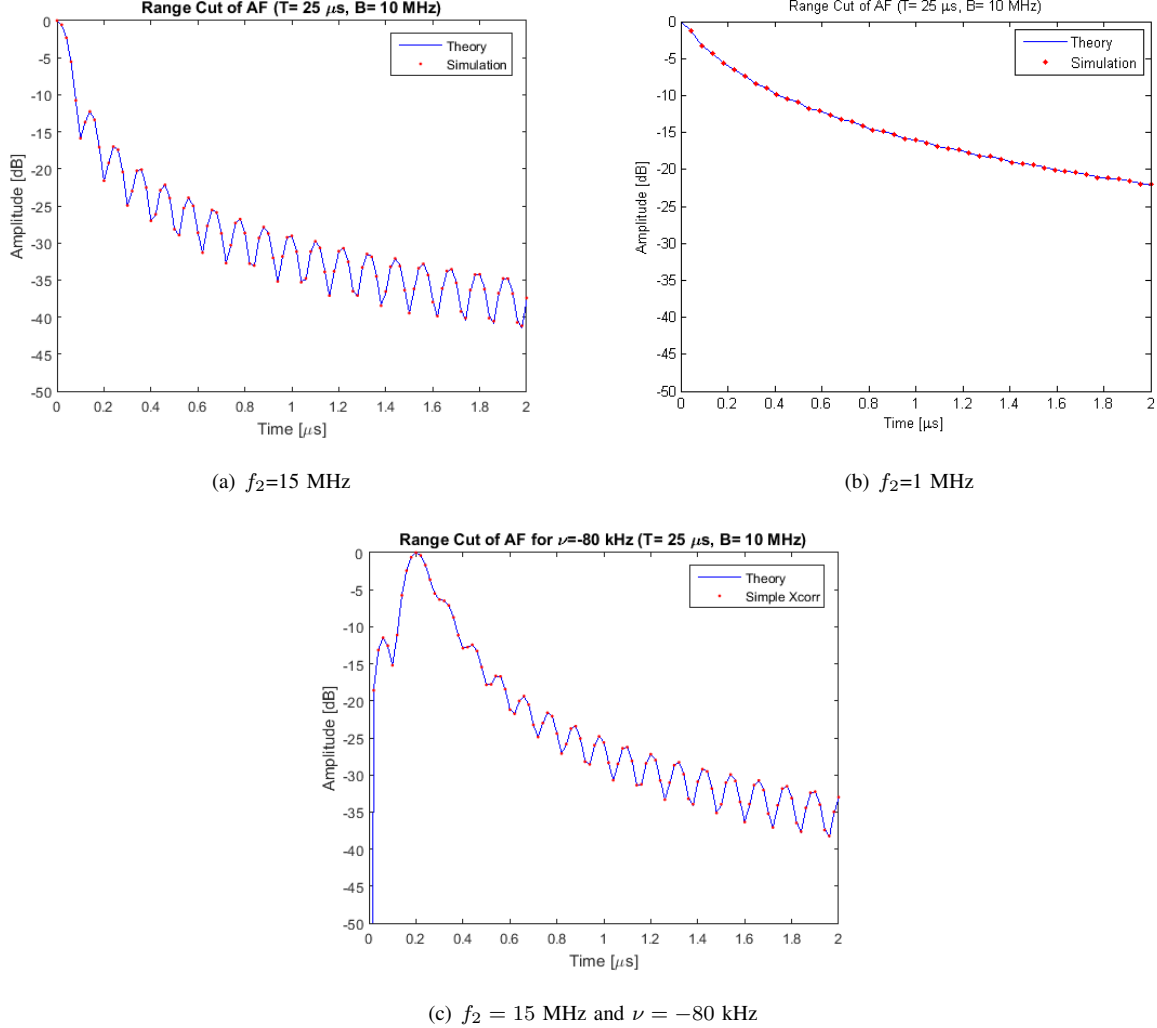


Fig. 2. Range Cut ($\nu = 0$) of the Ambiguity Function for a hyperbolic chirp with $T = 25 \mu s$, $B = 10$ MHz for a) $f_2 = 15$ MHz and b) $f_2 = 1$ MHz. Results show a very good agreement between theory (Eq. 10) and simulations. c) Cut of the Ambiguity Function relative to $\nu = -80$ kHz (corresponding to a product $\nu T = -2$) for $T = 25 \mu s$, $B = 10$ MHz and $f_2 = 15$ MHz. Results show a very good agreement between theory (Eq. 12 with 250 terms of the Taylor expansion) and simulations.

Fig. 2(a), Fig. 2(b) and Fig. 2(c) show the plots of the theoretical curves for $\nu = 0$ (i.e. the range cut of the Ambiguity Function) and for $\nu = -80$ kHz obtained by implementing Eq. 10 and Eq. 12 with 250 terms of the Taylor expansion. The curves are compared with the simulated cuts obtained by cross-correlating a delayed and frequency shifted replica of the transmitted chirp with the original transmitted version. Results show that there is a perfect agreement between the theoretical and simulated curves and prove the validity of the theoretical results. Results in Fig. 2(b) show that when f_2 becomes smaller than the bandwidth, and hence the condition on the parameters u and q is no longer satisfied, the shape and sidelobes of the range cut of the AF deteriorates. This is in agreement with what has been also observed in [7] and with simulations in [19].

III. MEASUREMENT ACCURACY OF TIME-DELAY AND DOPPLER

In this section, we study the accuracy of the joint estimates of time-delay and Doppler when a hyperbolic chirp is transmitted under the narrowband approximation for which the echo from a moving target is a delayed replica of the transmitted signal shifted in frequency. We calculate the Fisher Information Matrix (FIM), J_c , and find the CRLB of the estimators of the target position and target velocity.

It has been previously shown that the FIM can be written as

$$J_c = -2 \text{SNR } J_{AF} \quad (13)$$

where J_{AF} is the matrix of the second order derivatives of the squared amplitude of the CAF (see [20], [21], [22] and [23])

$$J_{AF} = \left(\begin{array}{cc} \frac{\partial^2 |\chi(\tau, \nu)|^2}{\partial \tau^2} & \frac{\partial^2 |\chi(\tau, \nu)|^2}{\partial \tau \partial \nu} \\ \frac{\partial^2 |\chi(\tau, \nu)|^2}{\partial \nu \partial \tau} & \frac{\partial^2 |\chi(\tau, \nu)|^2}{\partial \nu^2} \end{array} \right) \bigg|_{\tau, \nu=0}$$

To calculate the elements of the FIM for the hyperbolic chirp, we start by writing the second derivatives of the squared amplitude of the AF as a function of the first order and second order derivatives of the complex AF as

$$\frac{\partial^2 |\chi(\tau, \nu)|^2}{\partial \nu^2} = 2 \text{Real} \left\{ \chi^*(\tau, \nu) \frac{\partial^2 \chi(\tau, \nu)}{\partial \nu^2} \right\} + 2 \left| \frac{\partial \chi(\tau, \nu)}{\partial \nu} \right|^2 \quad (14)$$

$$\frac{\partial^2 |\chi(\tau, \nu)|^2}{\partial \tau^2} = 2 \text{Real} \left\{ \chi^*(\tau, \nu) \frac{\partial^2 \chi(\tau, \nu)}{\partial \tau^2} \right\} + 2 \left| \frac{\partial \chi(\tau, \nu)}{\partial \tau} \right|^2 \quad (15)$$

$$\frac{\partial^2 |\chi(\tau, \nu)|^2}{\partial \tau \partial \nu} = 2 \text{Real} \left\{ \chi^*(\tau, \nu) \frac{\partial \chi(\tau, \nu)}{\partial \tau \partial \nu} \right\} + 2 \text{Real} \left\{ \frac{\partial \chi^*(\tau, \nu)}{\partial \nu} \frac{\partial \chi(\tau, \nu)}{\partial \tau} \right\} \quad (16)$$

$$\frac{\partial^2 |\chi(\tau, \nu)|^2}{\partial \nu \partial \tau} = 2 \text{Real} \left\{ \chi^*(\tau, \nu) \frac{\partial \chi(\tau, \nu)}{\partial \nu \partial \tau} \right\} + 2 \text{Real} \left\{ \frac{\partial \chi(\tau, \nu)}{\partial \nu} \frac{\partial \chi^*(\tau, \nu)}{\partial \tau} \right\} \quad (17)$$

The derivatives with respect to ν can be easily calculated by deriving Eq. 8 with respect to ν and by considering that

$$\frac{d\beta}{d\nu} = j2\pi(T - \tau) \quad (18)$$

to obtain

$$\frac{\partial \chi(\tau, \nu)}{\partial \nu} = \frac{j2\pi(T - \tau)^2}{T(1 + k\tau)^{j2\pi a}} \int_0^1 w(1 - uw)^\gamma (1 - qw)^{-\gamma} e^{\beta w} dw \quad (19)$$

$$\frac{\partial^2 \chi(\tau, \nu)}{\partial^2 \nu} = \frac{-4\pi^2(T - \tau)^3}{T(1 + k\tau)^{j2\pi a}} \int_0^1 w^2(1 - uw)^\gamma (1 - qw)^{-\gamma} e^{\beta w} dw \quad (20)$$

For $(\tau, \nu = 0)$, we have $u = q = -kT$ and $\beta = 0$ and it can be easily shown that

$$\left. \frac{\partial \chi(\tau, \nu)}{\partial \nu} \right|_{\tau, \nu=0} = j\pi T \quad (21)$$

$$\left. \frac{\partial^2 \chi(\tau, \nu)}{\partial^2 \nu} \right|_{\tau, \nu=0} = -\frac{4}{3}\pi^2 T^2 \quad (22)$$

and hence, after applying Eq. 14, that

$$\left. \frac{\partial^2 |\chi(\tau, \nu)|^2}{\partial \nu^2} \right|_{\tau, \nu=0} = -\frac{2}{3}\pi^2 T^2 \quad (23)$$

The derivatives of the CAF with respect to ν in $(\tau, \nu = 0)$ do not depend on the waveform design and are the same for any types of waveform with unit energy and a rectangular amplitude modulation. This can be easily verified by deriving with respect to ν Eq. 4 rather than Eq. 8.

The derivatives of the AF with respect to τ are calculated by defining the function

$$u(t) = e^{j2\pi a \ln(1+kt)} = (1+kt)^{j2\pi a} \quad (24)$$

such that

$$\begin{cases} \frac{\partial u^*(t+\tau)}{\partial \tau} = -j2\pi a k [1+k(t+\tau)]^{-j2\pi a-1} \\ \frac{\partial^2 u^*(t+\tau)}{\partial \tau^2} = j2\pi a k^2 (1+j2\pi a) [1+k(t+\tau)]^{-j2\pi a-2} \end{cases} \quad (25)$$

The first order derivative with respect to τ is equal to (proof in Appendix B)

$$\begin{aligned} \frac{\partial \chi(\tau, \nu)}{\partial \tau} &= \frac{1}{T} \left[\int_0^{T-\tau} u(t) \frac{\partial u^*(t+\tau)}{\partial \tau} e^{j2\pi \nu t} dt - u(T-\tau) u^*(T) e^{j2\pi \nu (T-\tau)} \right] \\ &= \frac{1}{T} \left[-j2\pi a k \int_0^{T-\tau} (1+kt)^{j2\pi a} [1+k(t+\tau)]^{-j2\pi a-1} e^{j2\pi \nu t} dt \right. \\ &\quad \left. - [1+k(T-\tau)]^{j2\pi a} (1+kT)^{-j2\pi a} e^{j2\pi \nu (T-\tau)} \right] \end{aligned} \quad (26)$$

which for $\tau = 0$ and $\nu = 0$ simplifies to

$$\left. \frac{\partial \chi(\tau, \nu)}{\partial \tau} \right|_{\tau=0, \nu=0} = \frac{-j2\pi a}{T} \int_0^T \frac{k}{1+kt} dt - \frac{1}{T} = \frac{-j2\pi a \ln(1+kT) - 1}{T} \quad (27)$$

The second order derivative of the AF with respect to τ can be written as (Appendix B)

$$\begin{aligned} \frac{\partial^2 \chi(\tau, \nu)}{\partial \tau^2} &= \frac{1}{T} \left[\int_0^{T-\tau} u(t) \frac{\partial^2 u^*(t+\tau)}{\partial \tau^2} e^{j2\pi \nu t} dt - u(T-\tau) \left. \frac{\partial u^*(t+\tau)}{\partial \tau} \right|_{t=T-\tau} e^{j2\pi \nu (T-\tau)} \right. \\ &\quad \left. - u^*(T) \frac{\partial}{\partial \tau} (u(T-\tau) e^{j2\pi \nu (T-\tau)}) \right] \end{aligned} \quad (28)$$

and it is calculated by replacing $u(t)$ with Eq. 24 to obtain

$$\begin{aligned} \frac{\partial^2 \chi(\tau, \nu)}{\partial \tau^2} &= \frac{1}{T} \left[\int_0^{T-\tau} (1+kt)^{j2\pi a} j2\pi a k^2 (1+j2\pi a) [1+k(t+\tau)]^{-j2\pi a-2} e^{j2\pi \nu t} dt \right. \\ &\quad - [1+k(T-\tau)]^{j2\pi a} (-j2\pi a k) [1+kT]^{-j2\pi a-1} e^{j2\pi \nu (T-\tau)} \\ &\quad - (1+kT)^{-j2\pi a} (-j2\pi a k) [1+k(T-\tau)]^{j2\pi a-1} e^{j2\pi \nu (T-\tau)} \\ &\quad \left. + j2\pi \nu (1+kT)^{-j2\pi a} [1+k(T-\tau)]^{j2\pi a} e^{j2\pi \nu (T-\tau)} \right] \end{aligned} \quad (29)$$

For $\tau = 0$ and $\nu = 0$, the integral becomes

$$\left. \frac{\partial^2 \chi(\tau, \nu)}{\partial \tau^2} \right|_{\tau=0, \nu=0} = \frac{1}{T} \left[\int_0^T \frac{k^2(j2\pi a - 4\pi^2 a^2)}{(1+kt)^2} dt + \frac{j2\pi ak}{1+kT} + \frac{j2\pi ak}{1+kT} \right] \quad (30)$$

which after a simple calculation converges to

$$\left. \frac{\partial^2 \chi(\tau, \nu)}{\partial \tau^2} \right|_{\tau=0, \nu=0} = \frac{-4\pi^2 a^2 k^2}{1+kT} + j \frac{(2\pi a k^2 T + 4\pi a k)}{T(1+kT)} \quad (31)$$

The second derivatives of the squared amplitude of the AF with respect to τ can then be calculated as

$$\left. \frac{\partial^2 |\chi(\tau, \nu)|^2}{\partial \tau^2} \right|_{\tau=0, \nu=0} = \frac{-8\pi^2 a^2 k^2}{1+kT} + \frac{2+8\pi^2 a^2 \ln^2(1+kT)}{T^2} \quad (32)$$

To calculate $\frac{\partial^2 |\chi(\tau, \nu)|^2}{\partial \tau \partial \nu}$ we firstly observe that

$$2\text{Real} \left\{ \frac{\partial \chi(\tau, \nu)}{\partial \nu} \frac{\partial \chi^*(\tau, \nu)}{\partial \tau} \right\} = -4\pi^2 a \ln(1+kT) \quad (33)$$

We then take the derivative with respect to ν of Eq. 26

$$\begin{aligned} \frac{\partial \chi(\tau, \nu)}{\partial \tau \partial \nu} &= \frac{-j2\pi ak}{T} \int_0^{T-\tau} (j2\pi t)(1+kt)^{j2\pi a} [1+k(t+\tau)]^{-j2\pi a-1} e^{j2\pi \nu t} dt \\ &\quad - \frac{1}{T} [1+k(T-\tau)]^{j2\pi a} (1+kT)^{-j2\pi a} [j2\pi(T-\tau)] e^{j2\pi \nu(T-\tau)} \end{aligned} \quad (34)$$

and we calculate the results for $(\tau = 0, \nu = 0)$

$$\left. \frac{\partial^2 \chi(\tau, \nu)}{\partial \tau \partial \nu} \right|_{\tau=0, \nu=0} = \frac{4\pi^2 a}{T} \int_0^T \frac{kt}{1+kt} dt - j2\pi \quad (35)$$

$$\left. \frac{\partial^2 \chi(\tau, \nu)}{\partial \tau \partial \nu} \right|_{\tau=0, \nu=0} = \frac{4\pi^2 a}{T} \left[T - \frac{\ln(1+kT)}{k} \right] - j2\pi \quad (36)$$

$$2\text{Real} \left\{ \chi^*(\tau, \nu) \frac{\partial^2 \chi(\tau, \nu)}{\partial \tau \partial \nu} \right\} = 8\pi^2 a \left[1 - \frac{\ln(1+kT)}{kT} \right] \quad (37)$$

$$\left. \frac{\partial^2 |\chi(\tau, \nu)|^2}{\partial \tau \partial \nu} \right|_{\tau=0, \nu=0} = 8\pi^2 a \left[1 - \frac{\ln(1+kT)}{kT} \right] - 4\pi^2 a \ln(1+kT) \quad (38)$$

$$J_c = -2 \text{ SNR} \begin{pmatrix} \frac{-8\pi^2 a^2 k^2}{1+kT} + \frac{2+8\pi^2 a^2 \ln^2(1+kT)}{T^2} & 8\pi^2 a \left[1 - \frac{\ln(1+kT)}{kT} \right] - 4\pi^2 a \ln(1+kT) \\ 8\pi^2 a \left[1 - \frac{\ln(1+kT)}{kT} \right] - 4\pi^2 a \ln(1+kT) & -\frac{2}{3}\pi^2 T^2 \end{pmatrix} \quad (39)$$

The CRLB are the elements of the inverse of the matrix J_c and are equal to

$$CRLB(\tau) = -\frac{J_{AF}(2, 2)}{2 \text{ SNR } \det(J_{AF})} \quad (40)$$

$$CRLB(\nu) = -\frac{J_{AF}(1, 1)}{2 \text{ SNR } \det(J_{AF})} \quad (41)$$

IV. COMPARISON WITH THE MEASUREMENT ACCURACY OF THE LINEAR CHIRP

The calculations derived in Appendix B can equivalently be applied to the case of a linear chirp with a constant amplitude modulation $s(t) = \frac{1}{\sqrt{T}} e^{j\pi\gamma t^2} \text{Rect}\{t/T\}$ of duration T and bandwidth $B = \gamma T$. The FIM of a linear chirp is available in the literature [4] and it has previously been calculated by approximating the spectrum of the chirp with a rectangular shape for chirps with a large time-bandwidth product ($BT \gg 1$). Because the calculations developed in this paper, do not require the use of the Fourier Transform of the signal, a closed form solution can be obtained without the requirement for the signal to have a large time-bandwidth product. It can be shown (Proof in Appendix C) that the matrix of the second derivatives of the squared AF of a linear chirp can be written in the form

$$J_{AF_{linearchirp}} = \begin{pmatrix} -\frac{2}{3}\pi^2\gamma^2T^2 + \frac{2}{T^2} & \frac{2}{3}\pi^2\gamma T^2 \\ \frac{2}{3}\pi^2\gamma T^2 & -\frac{2}{3}\pi^2T^2 \end{pmatrix} \quad (42)$$

and by considering that $\gamma = B/T$ the results can be rewritten as

$$J_{AF_{linearchirp}} = -2 \begin{pmatrix} \frac{1}{3}\pi^2 \frac{(BT)^2 - 1}{T^2} & -2\pi \frac{\pi BT}{6} \\ -2\pi \frac{\pi BT}{6} & 4\pi^2 \frac{T^2}{12} \end{pmatrix} \quad (43)$$

For a chirp with a large time-bandwidth product ($BT \gg 1$) the element $J_{AF}(1,1) \cong \frac{1}{3}\pi^2 B^2$ and the matrix becomes of the form known in the literature [4]. It is straightforward to verify that the determinant of the matrix $J_{AF_{linearchirp}}$ is negative for small BT and that it is zero for $BT \gg 1$, meaning that the CRLBs do not exist for a single linear chirp. This result is well known in the existing literature; it can be easily shown that for only one pulse, at narrowband, the signal model for a linear chirp is not identifiable because the time-delay and the Doppler shift are coupled and cannot be uniquely estimated [4].

For completeness, the comparison is also extended to the case of a linear chirp with a Gaussian amplitude modulation

$$s(t) = \left(\frac{2k_G^2}{\pi}\right)^{1/4} e^{-k_G^2 t^2} e^{jb_G t^2} \quad (44)$$

and described by the parameters k_G and b_G . The parameter k_G is such that $k_G^2 = \frac{1}{2\lambda_G^2}$, where $2\lambda_G$ is the half power width of the Gaussian chirp envelope. The FIM of the Gaussian chirp is known in the literature [21] [24], and equal to

$$J_{AF_{GaussianChirp}} = -2 \begin{pmatrix} k_G^2 + \frac{b_G^2}{k_G^2} & \frac{\pi b_G}{k_G^2} \\ \frac{\pi b_G}{k_G^2} & \frac{\pi^2}{k_G^2} \end{pmatrix} \quad (45)$$

Fig. 3(a), Fig. 3(b) and Fig. 3(c) show the comparison in accuracy performance for a hyperbolic chirp and a Gaussian linear chirp of duration $25 \mu\text{s}$ and bandwidth 10 MHz (for the Gaussian chirp $2\lambda_G = 25 \mu\text{s}$). Results show that the CRLB of the hyperbolic chirp is about 3 dB lower than that of the Gaussian chirp for both time-delay and Doppler estimation. Results are similar for the lower bound of the cross-covariance between the estimators of the time-delay and the Doppler³. Similar results are obtained for the case $f_2 < B$.

³Care had to be taken in computing the elements of the FIM and the CRLB. Some of the elements can reach very small numbers and calculations can potentially compete with the current MATLAB[®] computational precision limits.

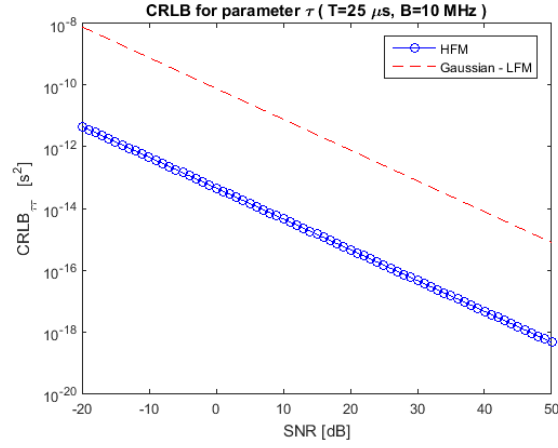
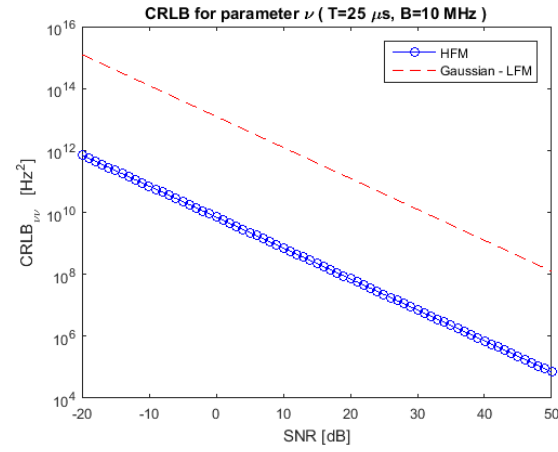
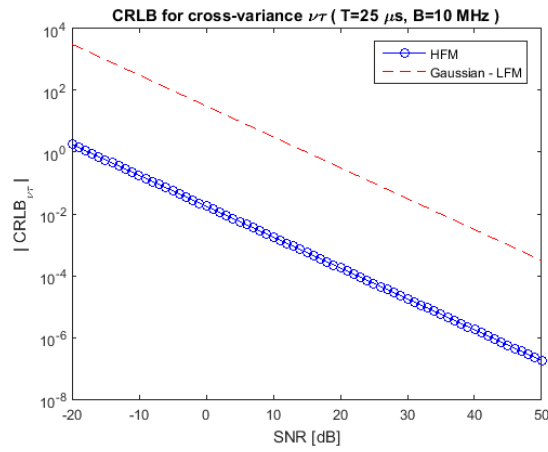
(a) CRLB for the time delay τ .(b) CRLB for the Doppler ν (c) Amplitude of the lower limit of the cross-variance between ν and τ .

Fig. 3. CRLB as a function of SNR for a) the time delay τ and b) the Doppler ν and c) amplitude of the lower limit of the cross-variance between ν and τ as a function of SNR.

V. ACCURACY OF A TRAIN OF TIME LIMITED PULSES

In this section, the calculations are extended to the case of a train of pulses of limited duration to allow the comparison with the accuracy of a rectangular linear chirp.

Consider a signal $s_N(t)$ of unit energy

$$s_N(t) = \frac{1}{\sqrt{N}} \sum_{n=0}^{N-1} s(t - nPRI) = \frac{1}{\sqrt{NT}} \sum_{n=0}^{N-1} u(t - nPRI) \text{Rect} \left\{ \frac{t - nPRI}{T} \right\} \quad (46)$$

consisting of a train of N pulses obtained by repeating the signal $s(t)$ with a Pulse Repetition Interval PRI such that $T < PRI$. To proceed with the calculations, we observe that the CAF $\chi_N(\tau, \nu)$ of the signal $s_N(t)$ can be written in the form [16]

$$\chi_N(\tau, \nu) = \chi(\tau, \nu) \frac{1}{N} \sum_{n=0}^{N-1} e^{j2\pi\nu nPRI} \quad (47)$$

and we proceed with calculating the matrix of the second derivatives of the squared amplitude of $\chi_N(\tau, \nu)$

$$J_{AFN} = \left(\begin{array}{cc} \frac{\partial^2 |\chi_N(\tau, \nu)|^2}{\partial \tau^2} & \frac{\partial^2 |\chi_N(\tau, \nu)|^2}{\partial \tau \partial \nu} \\ \frac{\partial^2 |\chi_N(\tau, \nu)|^2}{\partial \nu \partial \tau} & \frac{\partial^2 |\chi_N(\tau, \nu)|^2}{\partial \nu^2} \end{array} \right) \Big|_{\tau, \nu=0}$$

From Eq. 47, it is straight forward to observe that the first and second derivatives of $\chi_N(\tau, \nu)$ with respect to τ only depend on the term $\chi(\tau, \nu)$ and therefore that

$$\frac{\partial^2 |\chi_N(\tau, \nu)|^2}{\partial \tau^2} \Big|_{\tau, \nu=0} = \frac{\partial^2 |\chi(\tau, \nu)|^2}{\partial \tau^2} \Big|_{\tau, \nu=0} \quad (48)$$

It can be easily shown that the same applies to the cross derivatives with respect to τ and ν (Proof in Appendix D). To determine the second derivatives of the squared amplitude of $\chi_N(\tau, \nu)$ with respect to ν , we proceed by calculating the first and second derivatives of $\chi_N(\tau, \nu)$ in its complex form before using Eq. 15 to obtain the final results. From Eq. 47

$$\frac{\partial \chi_N(\tau, \nu)}{\partial \nu} = \frac{1}{N} \left[\frac{\partial \chi(\tau, \nu)}{\partial \nu} \sum_{n=0}^{N-1} e^{j2\pi\nu nPRI} + \chi(\tau, \nu) \sum_{n=0}^{N-1} j2\pi nPRI e^{j2\pi\nu nPRI} \right] \quad (49)$$

$$\frac{\partial \chi_N(\tau, \nu)}{\partial \nu} \Big|_{\tau, \nu=0} = \frac{\partial \chi(\tau, \nu)}{\partial \nu} \Big|_{\tau, \nu=0} + \frac{j2\pi PRI}{N} \chi(\tau, \nu) \Big|_{\tau, \nu=0} \sum_{n=0}^{N-1} n = \frac{\partial \chi(\tau, \nu)}{\partial \nu} \Big|_{\tau, \nu=0} + j\pi PRI(N-1) \quad (50)$$

Similarly, the second derivative of $\chi_N(\tau, \nu)$ in (0,0) is obtained by deriving Eq. 49 with respect to ν and by calculating its value in the origin.

$$\frac{\partial^2 \chi_N(\tau, \nu)}{\partial \nu^2} \Big|_{\tau, \nu=0} = \frac{1}{N} \left[\frac{\partial^2 \chi(\tau, \nu)}{\partial \nu^2} \Big|_{\tau, \nu=0} N + j4\pi PRI \frac{\partial \chi(\tau, \nu)}{\partial \nu} \Big|_{\tau, \nu=0} \sum_{n=0}^{N-1} n - 4\pi^2 PRI^2 \sum_{n=0}^{N-1} n^2 \right] \quad (51)$$

$$\frac{\partial^2 \chi_N(\tau, \nu)}{\partial \nu^2} \Big|_{\tau, \nu=0} = \frac{\partial^2 \chi(\tau, \nu)}{\partial \nu^2} \Big|_{\tau, \nu=0} + j4\pi PRI \frac{\partial \chi(\tau, \nu)}{\partial \nu} \Big|_{\tau, \nu=0} \frac{N-1}{2} - 4\pi^2 PRI^2 \frac{(N-1)(2N-1)}{6} \quad (52)$$

From the equation above, through a very simple calculation, it can be demonstrated that

$$\left. \frac{\partial^2 |\chi_N(\tau, \nu)|^2}{\partial \nu^2} \right|_{\tau, \nu=0} = \left. \frac{\partial^2 |\chi(\tau, \nu)|^2}{\partial \nu^2} \right|_{\tau, \nu=0} - \frac{2}{3} \pi^2 \text{PRI}^2 (N^2 - 1) \quad (53)$$

and hence that the matrix of the second derivatives of the squared amplitude of the ambiguity function is

$$J_{AF_N} = \left(\begin{array}{cc} \frac{\partial^2 |\chi(\tau, \nu)|^2}{\partial \tau^2} & \frac{\partial^2 |\chi(\tau, \nu)|^2}{\partial \tau \partial \nu} \\ \frac{\partial^2 |\chi(\tau, \nu)|^2}{\partial \nu \partial \tau} & -\frac{2}{3} \pi^2 T^2 - \frac{2}{3} \pi^2 \text{PRI}^2 (N^2 - 1) \end{array} \right) \bigg|_{\tau, \nu=0} \quad (54)$$

Similarly to the case of a single pulse, the CRLB for the time delay and the Doppler can be calculated as

$$\text{CRLB}(\tau) = -\frac{J_{AF_N}(2, 2)}{2 \text{SNR} \det(J_{AF_N})} \quad (55)$$

$$\text{CRLB}(\nu) = -\frac{J_{AF_N}(1, 1)}{2 \text{SNR} \det(J_{AF_N})} \quad (56)$$

Fig. 4(a), Fig. 4(b) and Fig. 4(c) show the CRLBs of a train of rectangular linear chirps and a train of hyperbolic chirps for a SNR of -10 dB. Each pulse has duration of 25 μs and a bandwidth of 10 MHz and the parameter f_2 of the hyperbolic chirp is 15 MHz. The energy of the signal in Eq. 46 is unity for any N and, similarly, the results are relative to a SNR which remains constant irrespective of the number of pulses forming the train. The results are given as a function of the number of pulses in a logarithmic scale and for $\text{PRI} = 1$ ms. Results show that the accuracy of the hyperbolic chirp and that of linear chirp is equal for both time, Doppler and for the cross-covariance of the two estimators. Results are similar for the case $f_2 < B$.

VI. COMPARISON BETWEEN NARROWBAND AFS

To understand the achieved accuracy results, we carry out a comparison of the AFs of the three types of waveform analysed in the previous sections. Fig. 5 and Fig. 6 show the ambiguity function of the three chirps of duration 25 μs and bandwidth 10 MHz together with their relative range and Doppler cuts. The plots in Fig.6(a) and Fig.6(b) show that there is a very close match between the Doppler and range cuts of the three waveforms. Because the FIM is a function of the second derivatives of the squared of the AF it is expected that similar shapes of the main AF lobe should lead to similar results in accuracy. Also, as it is well known in the existing literature, results show that the sidelobes of the Gaussian chirp are significantly lower and that the Doppler cuts of the rectangular linear chirp and hyperbolic chirp are equivalent. The results in Fig.5(a), Fig.5(b) and Fig.5(c) highlight that for narrowband processing the linear chirp is much more Doppler tolerant than the hyperbolic chirp. The narrowband approximation only accounts for a shift in frequency of the echo from a moving target. Whilst an echo shifted in frequency can be matched to a 0-Doppler reference signal by applying a simple time-delay for a linear frequency modulated chirp, this is not possible when the frequency modulation is hyperbolic. This phenomenon is nicely explained for the wideband case in [7] [8] and shown in Fig.7. Further results show that when the parameter f_2 increases and the bandwidth and the duration are fixed, and hence the hyperbolic chirp has a more linear transition in the time-frequency domain (see Fig. 1), the Doppler tolerance of the hyperbolic chirp also increases. These results indicate that it is possible to control the Doppler tolerance of the hyperbolic chirp by controlling the hyperbolic curvature via the parameter f_2 .

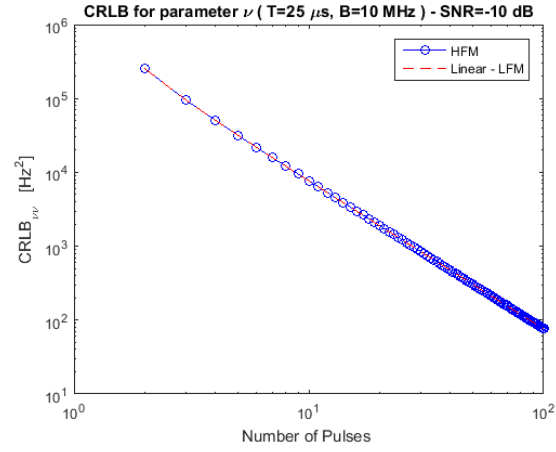
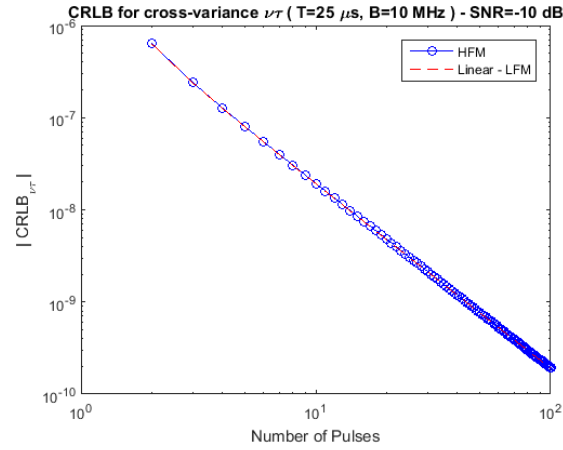
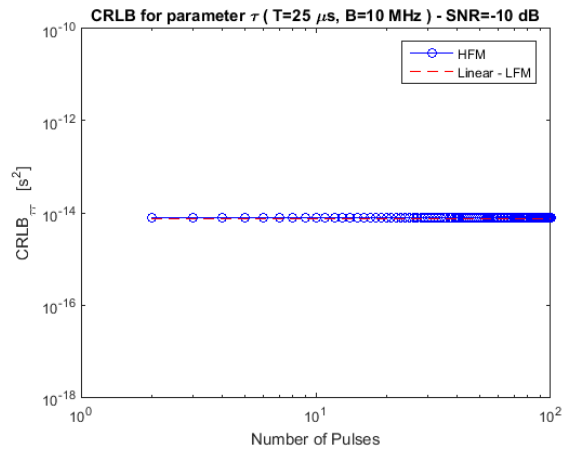
(a) CRLB for Doppler parameter ν (b) Amplitude of the lower limit of the cross-variance between ν and τ (c) CRLB for the time delay τ

Fig. 4. a) CRLB for the Doppler ν , b) amplitude of the lower limit of the cross-variance between ν and τ and c) CRLB for the time delay τ as a function of the number of pulses N (SNR = -10 dB and $PRI = 1$ ms).

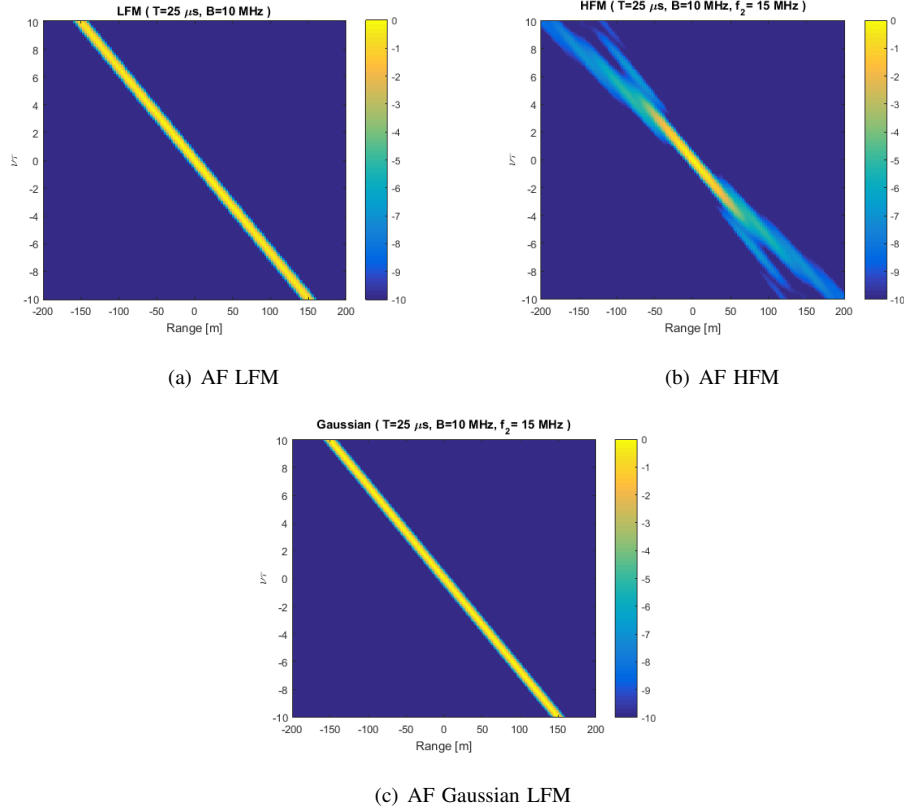


Fig. 5. Comparison between the ambiguity functions of a) a Linear Chirp, b) a Hyperbolic chirp ($f_2=15$ MHz) and c) a Gaussian chirp of bandwidth 10 MHz and duration $25 \mu s$.

VII. WIDEBAND AMBIGUITY FUNCTION

The analysis and the results of the previous sections are all based on the assumption of a narrowband signal for which an echo for a moving target is simply a delayed version of the transmitted signal but shifted in frequency of the Doppler shift $2v/c$, with v being the velocity of the target and c the speed of propagation of the waveform. It can be shown that the narrowband approximation is valid when $BT \ll c/(2v)$ ([20], pp. 241). However, there are applications of both radar and sonar for which the time-bandwidth product BT is not always significantly smaller than $c/(2v)$ and for which the narrowband approximation is no longer valid. For these applications, echoes from a moving target are characterised by a compression or expansion in the time domain that has to be taken into account in a matched receiver.

For these reasons, the Wideband Ambiguity Function (WAF) was proposed in [5] which is defined as

$$\chi(\tau, \nu) = \int_{-\infty}^{\infty} s(t) s^*[\nu(t + \tau)] dt \quad (57)$$

where $\nu = \frac{c-v}{c+v}$ is the Doppler compression factor. In this section, we derive the Wideband AF of the hyperbolic chirp and carry out a comparison with that of the linear chirp in order to draw differences and similarities with respect to the narrowband case. An approximation of the WAF of the hyperbolic chirp obtained using a second

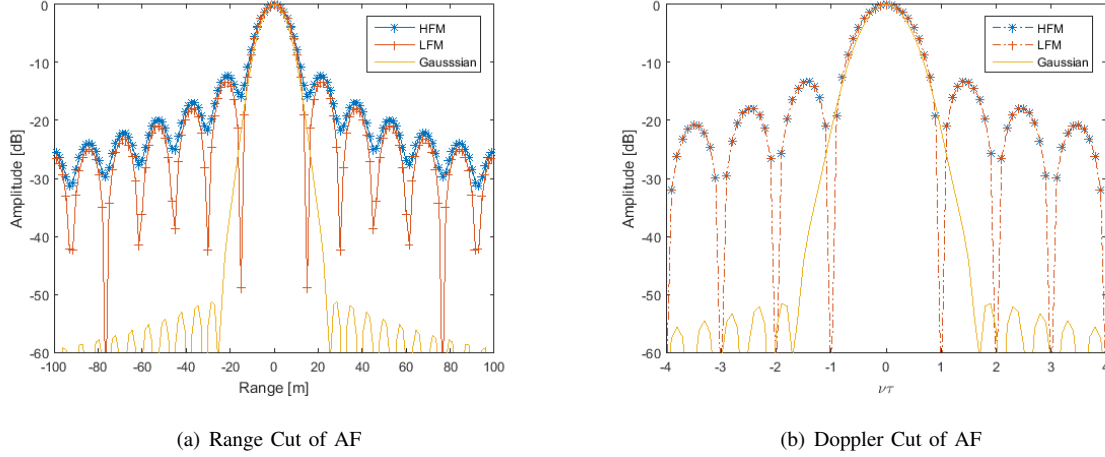


Fig. 6. Comparison between the a) Range cuts and b) Doppler cuts of a Linear Chirp, a Hyperbolic chirp ($f_2=15$ MHz) and a Gaussian chirp of bandwidth 10 MHz and duration $25 \mu s$.

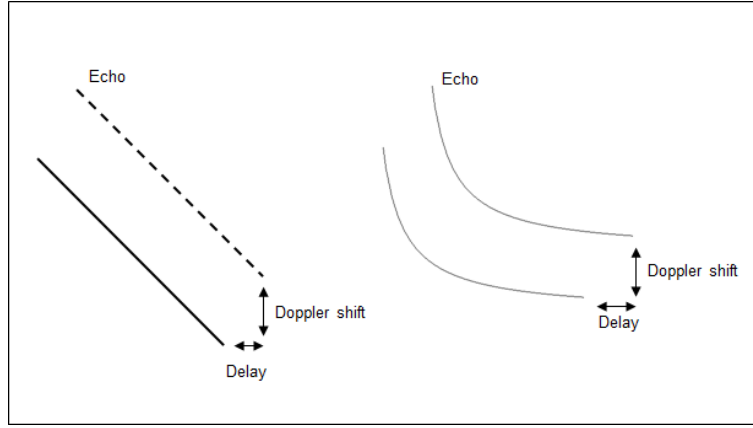


Fig. 7. Linear and hyperbolic chirps with relative echoes shifted in Doppler. In the presence of a Doppler mismatch, a time translation by a narrowband cross-correlation receiver can provide a strong overlap between the echo and the transmitted signals in the case of a linear chirp. This is not possible for a hyperbolic chirp.

order Taylor expansion has been previously derived and is available in [6]. The calculations are carried out for $\tau > 0$ with no loss of generality for the case of a time compression ($\nu > 1$) and a time expansion ($\nu < 1$) as

$$\chi(\tau, \nu \geq 1) = \begin{cases} \frac{1}{T} \int_0^{\frac{T}{\nu}-\tau} (1+kt)^{j2\pi a} (1+k\nu[t+\tau])^{-j2\pi a} dt & 0 < \tau < \frac{T}{\nu} \\ 0 & \tau > \frac{T}{\nu} \end{cases} \quad (58)$$

$$\chi(\tau, \nu < 1) = \begin{cases} \frac{1}{T} \int_0^T (1+kt)^{j2\pi a} (1+k\nu[t+\tau])^{-j2\pi a} dt & 0 < \tau < \frac{T}{\nu} - T \\ \frac{1}{T} \int_0^{\frac{T}{\nu}-\tau} (1+kt)^{j2\pi a} (1+k\nu[t+\tau])^{-j2\pi a} dt & \frac{T}{\nu} - T < \tau < \frac{T}{\nu} \\ 0 & \tau > \frac{T}{\nu} \end{cases} \quad (59)$$

The integrals are calculated similarly to the CAF of the narrowband signal. The integral in the interval $[0, \frac{T}{\nu} - \tau]$ is solved by the two changes of variable $t_1 = kt$ and $t_1 = k(\frac{T}{\nu} - \tau)w$ and by defining the parameters

$$\begin{cases} \gamma = j2\pi a \\ u = k(-\frac{T}{\nu} + \tau) \\ q = \frac{k(\nu\tau - T)}{1 + k\nu\tau} \end{cases}$$

to lead to the final result

$$\chi(\tau, \nu) = \frac{\nu^{-\gamma}}{T} \left(\frac{T}{\nu} - \tau \right) \left(\frac{k\nu\tau + 1}{\nu} \right)^{-j2\pi a} F_1(1, -\gamma, \gamma, 2; u, q) \quad (60)$$

Similarly, the integral in the interval $[0, T]$ is calculated with a simple change of variable $t = t_1 T$ and by defining the parameters

$$\begin{cases} \gamma = j2\pi a \\ u_1 = -kT \\ q_1 = \frac{-k\nu T}{1 + k\nu\tau} \end{cases}$$

to obtain the final result

$$\chi(\tau, \nu) = (1 + k\nu\tau)^{-j2\pi a} F_1(1, -\gamma, \gamma, 2; u_1, q_1) \quad (61)$$

Fig. 8(a) shows the theoretical AF for a ultrasound hyperbolic chirp of duration $T = 3$ ms, bandwidth $B = 20$ kHz and lower frequency $f_2 = 30$ kHz for $\nu = 1.05$ compared to the same simulated cut. Because the speed of sound in air is much lower than the speed of light, the narrowband approximation does not hold and wideband processing is required despite $BT = 60$. Results show a perfect match between theory and simulation proving the validity of the theoretical results. Fig. 8(b) and Fig. 8(c) show a comparison between the WAF of the same hyperbolic chirp and that of a linear chirp of the same bandwidth $B = 20$ kHz and duration $T = 3$ ms. Fig. 8(d) shows a comparison between the range cuts for $\nu = 1.05$. Results clearly show that at wideband, as expected, the hyperbolic chirp is more Doppler tolerant than the linear chirp. This property of the hyperbolic chirp is well known in the literature and some key recommended references are [7] and [8].

VIII. CONCLUSIONS

In this paper, we have derived the expressions of the AF of a narrowband and a wideband hyperbolic chirp. We have calculated the second derivatives of the squared amplitude of the narrowband CAF and the elements of the FIM of the estimators of the target range and velocity and their CRLBs. We have also presented an analysis of estimation performance and a comparison with the case of a linear chirp with a rectangular and a Gaussian amplitude modulations. Results have corroborated that, at narrowband, the linear chirp is more Doppler tolerant than the hyperbolic chirp. The analysis of the CRLBs has demonstrated that the accuracy of the hyperbolic chirp at narrowband is about 3 dB better than that of the Gaussian chirp and comparable to that of a train of linear chirps with constant amplitude modulation. The results of the WAF have corroborated the superior Doppler tolerance of the hyperbolic chirp at wideband. The main equations derived in this paper are a) Eq. 10 and Eq. 12 give the narrowband AF of the hyperbolic chirp, b) Eq. 39 gives the FIM of the hyperbolic chirp, c) Eq. 42 gives the FIM

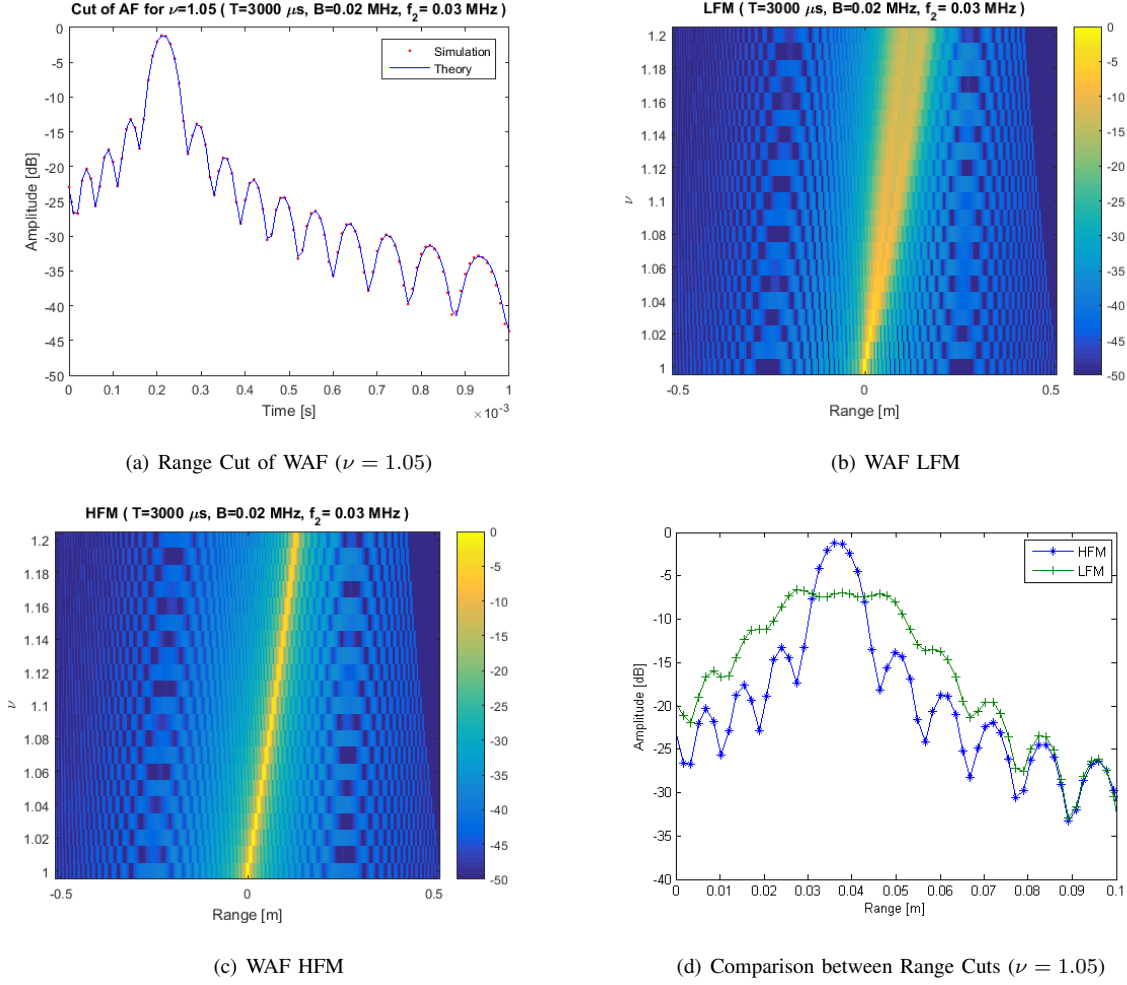


Fig. 8. a) Theoretical and simulated range cut ($\nu = 1.05$) of the WAF for a hyperbolic chirp ($f_2=30$ kHz) and comparison between the WAFs of b) a linear chirp and c) a hyperbolic chirp ($f_2=30$ kHz) and d) between the range cuts for $\nu = 1.05$. Results are relative to signals with a duration $T = 3$ ms and a bandwidth $B = 20$ kHz.

for the linear chirp for any time-bandwidth products, d) Eq. 54 gives the FIM for a train of pulses and e) Eq. 60 and Eq. 61 give the wideband AF of the hyperbolic chirp.

APPENDIX A

TABLED INTEGRAL - HYPERGEOMETRIC FUNCTION (PP. 287)

$$\int_0^1 x^{\lambda-1} (1-x)^{\mu-1} (1-ux)^{-\rho} (1-vx)^{-\sigma} dx = \mathbf{B}(\mu, \lambda) F_1(\lambda, \rho, \sigma, \lambda + \mu; u, v) \quad (62)$$

APPENDIX B

PROOF OF THE DERIVATIVES WITH RESPECT TO THE PARAMETER τ

$$\psi(\tau, \nu) = \frac{1}{T} \int_{-\infty}^{\infty} u(t) \text{Rect} \left\{ \frac{t}{T} \right\} g^*(t + \tau) \text{Rect} \left\{ \frac{t + \tau}{T} \right\} e^{j2\pi\nu t} dt \quad (63)$$

$$\frac{\partial \psi(\tau, \nu)}{\partial \tau} = \frac{1}{T} \int_{-\infty}^{\infty} u(t) \text{Rect} \left\{ \frac{t}{T} \right\} \frac{\partial}{\partial \tau} \left(g^*(t + \tau) \text{Rect} \left\{ \frac{t + \tau}{T} \right\} \right) e^{j2\pi \nu t} dt \quad (64)$$

$$\frac{\partial (g^*(t + \tau) \text{Rect} \left\{ \frac{t + \tau}{T} \right\})}{\partial \tau} = \frac{\partial g^*(t + \tau)}{\partial \tau} \text{Rect} \left\{ \frac{t + \tau}{T} \right\} + g^*(t + \tau) [\delta(t + \tau) - \delta(t - T + \tau)] \quad (65)$$

$$\begin{aligned} \frac{\partial \psi(\tau, \nu)}{\partial \tau} = & \frac{1}{T} \int_{-\infty}^{\infty} u(t) \text{Rect} \left\{ \frac{t}{T} \right\} \frac{\partial g^*(t + \tau)}{\partial \tau} \text{Rect} \left\{ \frac{t + \tau}{T} \right\} e^{j2\pi \nu t} dt \\ & + \frac{1}{T} \int_{-\infty}^{\infty} u(t) g^*(t + \tau) \text{Rect} \left\{ \frac{t}{T} \right\} [\delta(t + \tau) - \delta(t - T + \tau)] e^{j2\pi \nu t} dt \end{aligned} \quad (66)$$

For $0 < \tau < T$ the term $\text{Rect} \left\{ \frac{-\tau}{T} \right\} = 0$ and the equation becomes

$$\frac{\partial \psi(\tau, \nu)}{\partial \tau} = \frac{1}{T} \int_{-\infty}^{\infty} u(t) \text{Rect} \left\{ \frac{t}{T} \right\} \frac{\partial g^*(t + \tau)}{\partial \tau} \text{Rect} \left\{ \frac{t + \tau}{T} \right\} e^{j2\pi \nu t} dt - \frac{1}{T} u(T - \tau) g^*(T) e^{j2\pi \nu (T - \tau)} \quad (67)$$

We also note that the integral term in Eq. 67 is of the same form of that in Eq. 63 and hence the same property can be used to calculate the higher order derivatives of the complex AF with respect to τ . In the specific case of the AF, $g(t) = u(t)$ and

$$\frac{\partial \chi(\tau, \nu)}{\partial \tau} = \frac{1}{T} \int_0^{T - \tau} u(t) \frac{\partial u^*(t + \tau)}{\partial \tau} e^{j2\pi \nu t} dt - \frac{1}{T} u(T - \tau) u^*(T) e^{j2\pi \nu (T - \tau)} \quad (68)$$

$$\begin{aligned} \frac{\partial^2 \chi(\tau, \nu)}{\partial \tau^2} = & \frac{1}{T} \int_0^{T - \tau} u(t) \frac{\partial^2 u^*(t + \tau)}{\partial \tau^2} e^{j2\pi \nu t} dt - \frac{1}{T} u(T - \tau) \left. \frac{\partial u^*(t + \tau)}{\partial \tau} \right|_{t=T - \tau} e^{j2\pi \nu (T - \tau)} \\ & - \frac{1}{T} u^*(T) \frac{\partial}{\partial \tau} (u(T - \tau) e^{j2\pi \nu (T - \tau)}) \end{aligned} \quad (69)$$

APPENDIX C

ELEMENTS OF THE FIM OF A LINEAR CHIRP

$$u(t) = e^{j\pi \gamma t^2} \quad (70)$$

$$u^*(t + \tau) = e^{-j\pi \gamma (t + \tau)^2} \quad (71)$$

$$\frac{\partial u^*(t + \tau)}{\partial \tau} = -j2\pi \gamma (t + \tau) e^{-j\pi \gamma (t + \tau)^2} \quad (72)$$

$$\frac{\partial^2 u^*(t + \tau)}{\partial \tau^2} = -j2\pi \gamma e^{-j\pi \gamma (t + \tau)^2} - 4\pi^2 \gamma^2 (t + \tau)^2 e^{-j\pi \gamma (t + \tau)^2} \quad (73)$$

$$a = \frac{1}{T} u(T - \tau) \left. \frac{\partial u^*(t + \tau)}{\partial \tau} \right|_{t=T - \tau} e^{j2\pi \nu (T - \tau)} = -j2\pi \gamma e^{j\pi \gamma (T - \tau)^2} e^{-j\pi \gamma T^2} e^{j2\pi \nu (T - \tau)} \quad (74)$$

$$a|_{\tau, \nu=0} = -j2\pi \gamma \quad (75)$$

$$b = \frac{1}{T} u^*(T) \frac{\partial}{\partial \tau} \left(u(T - \tau) e^{j2\pi\nu(T-\tau)} \right) = \frac{1}{T} e^{-j\pi\gamma T^2} \frac{\partial}{\partial \tau} \left[e^{j\pi\gamma(T-\tau)^2} e^{j2\pi\nu(T-\tau)} \right] \quad (76)$$

$$b = \frac{1}{T} e^{-j\pi\gamma T^2} \left(-j2\pi\nu e^{j2\pi\nu(T-\tau)} e^{j\pi\gamma(T-\tau)^2} - j2\pi\gamma(T-\tau) e^{j2\pi\nu(T-\tau)} e^{j\pi\gamma(T-\tau)^2} \right) \quad (77)$$

$$b|_{\tau,\nu=0} = e^{-j\pi\gamma T^2} \left(-j2\pi\gamma e^{j\pi\gamma T^2} \right) = -j2\pi\gamma \quad (78)$$

$$c = \frac{1}{T} \int_0^{T-\tau} u(t) \frac{\partial^2 u^*(t+\tau)}{\partial \tau^2} e^{j2\pi\nu t} dt \quad (79)$$

$$c = \frac{1}{T} \int_0^{T-\tau} e^{j\pi\gamma t^2} \left[-j2\pi\gamma e^{-j\pi\gamma(t+\tau)^2} - 4\pi^2\gamma^2(t+\tau)^2 e^{-j\pi\gamma(t+\tau)^2} \right] e^{j2\pi\nu t} dt \quad (80)$$

$$c|_{\tau,\nu=0} = \frac{1}{T} \int_0^T (-j2\pi\gamma - 4\pi^2\gamma^2 t^2) dt = -j2\pi\gamma - \frac{4}{3}\pi^2\gamma^2 T^2 \quad (81)$$

$$\left. \frac{\partial^2 \chi(\tau, \nu)}{\partial \tau^2} \right|_{\tau,\nu=0} = c - a - b = -\frac{4}{3}\pi^2\gamma^2 T^2 + j2\pi\gamma \quad (82)$$

$$\frac{\partial \chi(\tau, \nu)}{\partial \tau} = \frac{1}{T} \int_0^{T-\tau} e^{j\pi\gamma t^2} \left[-j2\pi\gamma(t+\tau) e^{j\pi\gamma(t+\tau)^2} \right] e^{j2\pi\nu t} dt - \frac{1}{T} e^{j\pi\gamma(T-\tau)^2} e^{j\pi\gamma T^2} e^{j2\pi\nu(T-\tau)} \quad (83)$$

$$\left. \frac{\partial \chi(\tau, \nu)}{\partial \tau} \right|_{\tau,\nu=0} = \frac{1}{T} \int_0^T -j2\pi\gamma t dt - \frac{1}{T} = -j\pi\gamma T - \frac{1}{T} \quad (84)$$

Using Eq. 15 it is possible to calculate the second derivative of the squared amplitude of the CAF with respect to τ as

$$\left. \frac{\partial^2 |\chi(\tau, \nu)|^2}{\partial \tau^2} \right|_{\tau,\nu=0} = -\frac{8}{3}\pi^2\gamma^2 T^2 + 2 \left(\pi^2\gamma^2 T^2 + \frac{1}{T^2} \right) = -\frac{2}{3}\pi^2\gamma^2 T^2 + \frac{2}{T^2} \quad (85)$$

$$\frac{\partial^2 \chi(\tau, \nu)}{\partial \tau \partial \nu} = \frac{1}{T} \int_0^{T-\tau} j2\pi t e^{j\pi\gamma t^2} \left[-j2\pi\gamma(t+\tau) e^{j\pi\gamma(t+\tau)^2} \right] e^{j2\pi\nu t} dt - \frac{1}{T} j2\pi(T-\tau) e^{j\pi\gamma(T-\tau)^2} e^{j\pi\gamma T^2} e^{j2\pi\nu(T-\tau)} \quad (86)$$

$$\left. \frac{\partial^2 \chi(\tau, \nu)}{\partial \tau \partial \nu} \right|_{\tau,\nu=0} = \frac{1}{T} \int_0^T 4\pi^2\gamma t^2 dt - j2\pi = \frac{4}{3}\pi^2\gamma T^2 - j2\pi \quad (87)$$

$$\left. \frac{\partial^2 |\chi(\tau, \nu)|^2}{\partial \tau \partial \nu} \right|_{\tau,\nu=0} = \frac{8}{3}\pi^2\gamma T^2 + 2\text{Real} \left\{ -j\pi T \left(-j\pi\gamma T - \frac{1}{T} \right) \right\} = \frac{2}{3}\pi^2\gamma T^2 \quad (88)$$

APPENDIX D

PROOF OF CROSS SECOND ORDER DERIVATIVES FOR A TRAIN OF PULSES

To evaluate the cross derivatives of $\chi_N(\tau, \nu)$, we first derive Eq. 47 with respect to the parameter τ and then with respect to ν

$$\frac{\partial \chi_N(\tau, \nu)}{\partial \tau} = \frac{\partial \chi(\tau, \nu)}{\partial \tau} \frac{1}{N} \sum_{n=0}^{N-1} e^{j2\pi \nu n PRI} \quad (89)$$

$$\frac{\partial^2 \chi_N(\tau, \nu)}{\partial \tau \partial \nu} = \frac{\partial \chi(\tau, \nu)}{\partial \tau \partial \nu} \frac{1}{N} \sum_{n=0}^{N-1} e^{j2\pi \nu n PRI} + \frac{\partial \chi(\tau, \nu)}{\partial \tau} \frac{1}{N} \sum_{n=0}^{N-1} j2\pi n PRI e^{j2\pi \nu n PRI} \quad (90)$$

These quantities in the origin are equal to

$$\left. \frac{\partial \chi_N(\tau, \nu)}{\partial \tau} \right|_{\tau, \nu=0} = \left. \frac{\partial \chi(\tau, \nu)}{\partial \tau} \right|_{\tau, \nu=0} \quad (91)$$

$$\left. \frac{\partial \chi_N(\tau, \nu)}{\partial \tau \partial \nu} \right|_{\tau, \nu=0} = \left. \frac{\partial \chi(\tau, \nu)}{\partial \tau \partial \nu} \right|_{\tau, \nu=0} + j2\pi PRI \frac{N-1}{2} \left. \frac{\partial \chi(\tau, \nu)}{\partial \tau} \right|_{\tau, \nu=0} \quad (92)$$

We can then apply Eq. 16 and use the result in Eq. 91 and Eq. 92 to write

$$\begin{aligned} \left. \frac{\partial |\chi_N(\tau, \nu)|^2}{\partial \tau \partial \nu} \right|_{\tau, \nu=0} &= 2\text{Real} \left\{ \left. \frac{\partial \chi(\tau, \nu)}{\partial \tau \partial \nu} \right|_{\tau, \nu=0} + j2\pi PRI \frac{N-1}{2} \left. \frac{\partial \chi(\tau, \nu)}{\partial \tau} \right|_{\tau, \nu=0} \right\} + \\ &2\text{Real} \left\{ \left. \frac{\partial \chi(\tau, \nu)}{\partial \tau} \right|_{\tau, \nu=0} \left(\left. \frac{\partial \chi^*(\tau, \nu)}{\partial \nu} \right|_{\tau, \nu=0} - j\pi PRI(N-1) \right) \right\} = \\ &\left. \frac{\partial |\chi(\tau, \nu)|^2}{\partial \tau \partial \nu} \right|_{\tau, \nu=0} \end{aligned} \quad (93)$$

ACKNOWLEDGMENT

The authors would like to thank Professor Fulvio Gini for referring them to references [9], [10] and [11] and Professor Hugh Griffiths for suggesting reference [7]. Alessio Balleri would like to thank Dr Venkat Sastry for their interesting discussions on the convergence of the Hypergeometric functions and for referring him to reference [17].

REFERENCES

- [1] E. Kelly, "The radar measurement of range, velocity and acceleration," *IRE Transactions on Military Electronics*, vol. MIL-5, no. 2, pp. 51–57, April 1961.
- [2] P. Bello, "Joint estimation of delay, Doppler, and Doppler rate," *IRE Transactions on Information Theory*, vol. 6, no. 3, pp. 330–341, June 1960.
- [3] A. Swindlehurst and P. Stoica, "Maximum likelihood methods in radar array signal processing," *Proceedings of the IEEE*, vol. 86, no. 2, pp. 421–441, Feb 1998.
- [4] A. Dogandzic and A. Nehorai, "Cramer-Rao bounds for estimating range, velocity, and direction with an active array," *IEEE Transactions on Signal Processing*, vol. 49, no. 6, pp. 1122–1137, Jun 2001.
- [5] E. Kelly and R. Wishner, "Matched-filter theory for high-velocity, accelerating targets," *IEEE Transactions on Military Electronics*, vol. 9, no. 1, pp. 56–69, Jan 1965.
- [6] A. Rihaczek, "Doppler-tolerant signal waveforms," *Proceedings of the IEEE*, vol. 54, no. 6, pp. 849–857, June 1966.
- [7] J. Kroszczynski, "Pulse compression by means of linear-period modulation," *Proceedings of the IEEE*, vol. 57, no. 7, pp. 1260–1266, July 1969.
- [8] C. J. Kiss, "Hyperbolic- FM (CHYPE)," Army Missile Command, Redstone Arsenal, Alabama, AD-771 046, Tech. Rep., 1973.

- [9] O. Besson, G. Giannakis, and F. Gini, "Fast and accurate estimation of hyperbolic frequency modulated chirp signals," in *Fourth International Conference on Signal Processing Proceedings, 1998. ICSP '98.*, 1998, pp. 148–151 vol.1.
- [10] F. Gini and G. Giannakis, "Hybrid FM-polynomial phase signal modeling: parameter estimation and Cramer-Rao bounds," *IEEE Transactions on Signal Processing*, vol. 47, no. 2, pp. 363–377, Feb 1999.
- [11] O. Besson, G. Giannakis, and F. Gini, "Improved estimation of hyperbolic frequency modulated chirp signals," *IEEE Transactions on Signal Processing*, vol. 47, no. 5, pp. 1384–1388, May 1999.
- [12] M. Vespe, G. Jones, and C. Baker, "Lessons for radar," *Signal Processing Magazine, IEEE*, vol. 26, no. 1, pp. 65–75, Jan 2009.
- [13] P. Flandrin, *Animal Sonar: Processes and Performance*. Boston, MA: Springer US, 1988, ch. Time-Frequency Processing of Bat Sonar Signals, pp. 797–802.
- [14] F. Hlawatsch and G. F. Boudreaux-Bartels, "Linear and quadratic time-frequency signal representations," *IEEE Signal Processing Magazine*, vol. 9, no. 2, pp. 21–67, April 1992.
- [15] A. Farina, "Cognitive Radar Signal Processing," *Key Note Speech, IET International Radar Conference, Hangzhou, China*, 14-16 Oct. 2015.
- [16] N. Levanon and E. Mozeson, *Radar Signals*. Wiley, 2004.
- [17] I. S. Gradshteyn and I. M. Ryzhik, *Table of integrals, series, and products*. Academic Press, 1980.
- [18] W. Bailey, *Appell's Hypergeometric Functions of Two Variables (Ch. 9 in Generalised Hypergeometric Series)*. Cambridge University Press, 1935.
- [19] C. Baker, H. Griffiths, and A. Balleri, "Biologically inspired waveform diversity (in Waveform Design and Diversity for Advanced Radar Systems)," *Institution of Engineering and Technology, Series on Radar, Sonar, Navigation and Avionics*, pp. 149–172, 2012.
- [20] H. L. Van Trees, *Detection, estimation and modulation theory, Part III. Radar-Sonar signal processing and Gaussian signals in noise*. Wiley, 2001.
- [21] C. E. Cook and M. Bernfeld, *Radar Signals: an introduction to theory and application*. Artech House, 1987.
- [22] M. Greco, P. Stinco, F. Gini, and A. Farina, "Cramer-Rao bounds and selection of bistatic channels for multistatic radar systems," *IEEE Transactions on Aerospace and Electronic Systems*, vol. 47, no. 4, pp. 2934–2948, October 2011.
- [23] P. Stinco, M. Greco, F. Gini, and M. Rangaswamy, "Ambiguity function and Cramer-Rao bounds for universal mobile telecommunications system-based passive coherent location systems," *IET Radar, Sonar Navigation*, vol. 6, no. 7, pp. 668–678, August 2012.
- [24] D. Kershaw and R. Evans, "Optimal waveform selection for tracking systems," *IEEE Transactions on Information Theory*, vol. 40, no. 5, pp. 1536–1550, Sep 1994.

Ambiguity function and accuracy of the hyperbolic chirp: comparison with the linear chirp

Balleri, Alessio

2016-07-06

Attribution-NonCommercial 4.0 International

Balleri A, Farina A. (2017) Ambiguity function and accuracy of the hyperbolic chirp: comparison with the linear chirp, IET Radar Sonar and Navigation, Volume 11, Issue 1, 2017, pp. 142-153

<http://dx.doi.org/10.1049/iet-rsn.2016.0100>

Downloaded from CERES Research Repository, Cranfield University